

Modeling and Estimation of Servo Actuator Dynamic Variability with Application to LTO-drives

Longhao Wang and Raymond A. de Callafon

Abstract—Starting from multiple frequency domain measurements, this paper presents a procedure to formulate a dynamic model of a servo actuator that consists of a nominal model and an allowable model perturbation in the form of a parametric and unstructured uncertainty. A separation between parametric and unstructured uncertainty is achieved by first estimating low order linear parameter models via frequency domain curve fitting followed by a linear Principle Component Analysis (PCA) to bound the parametric variations on the estimated parameters. Remaining differences between the low order parametric models and the measured frequency responses are captured by a bounded unstructured uncertainty on a frequency dependent dual-Youla parameter that uses prior information on a stabilizing feedback controller. The resulting perturbation model is written in a standard Linear Fractional Transformation (LFT) form and the procedure is applied to experimental data obtained from several mechanically equivalent servo actuators in a Linear Tape Open (LTO) drive.

I. INTRODUCTION

Manufacturing variability, temperature and position dependency will cause variations in the dynamic behavior of a servo actuator and modern robust control design approaches [1], [2] could potentially compensate for such variations. However, for guaranteeing stability and performance robustness a so-called perturbation or uncertainty model is needed to model and bound the variations in the dynamic behavior of a servo actuator.

Convex approaches to estimating low order models with uncertainty [3] require strong assumptions on the noise on the data. Using frequency domain data to formulate bounds on model uncertainty optimal for control design is well documented in [4] but may lead to models with high complexity when combined with optimal H_∞ bounds. Uncertainty modeling of low complexity models from experimental data is often rephrased as a model validation problem [5], [6], but requires the formulation of a nominal model and uncertainty bounds *a priori*. Estimating uncertainty models for flexible structures have been reported for aerospace applications [7] and more recently for (dual stage) servo actuators in magnetic hard disk drives [8], [9] where frequency domain measurements are used to formulate bounds on actuator variability.

The uncertainty modeling should be aimed at separating structured and unstructured variations in the dynamics [10].

This work was supported by the INSIC TAPE program.

L. Wang is a graduate student with the Dept. of Mechanical and Aerospace Engineering, University of California, San Diego, 9500 Gilman Dr., La Jolla, CA 92093-0411, U.S.A. l3wang@ucsd.edu

R.A. de Callafon is a Professor with the Dept. of Mechanical and Aerospace Engineering, University of California, San Diego, 9500 Gilman Dr., La Jolla, CA 92093-0411, U.S.A. callafon@ucsd.edu

In particular for servo actuators, structured variations are used to capture real-valued parametric variations in gain, location and damping of resonance modes. Complex unstructured variations are used to bound non-structural variations measured in the frequency response. This separation is even more important for high performance control of servo actuators in Linear Tape Open (LTO) drives [11], [12] where frequency domain measurements are readily available for modeling purposes [13]. In LTO drives structural variations are mainly due to variations in manufacturing, while unstructured variations occur due to the exchange of different tape cartridges and the inherent tape/head interaction.

Starting from multiple frequency domain measurements obtained from LTO servo actuators [14], this paper presents a modeling procedure to formulate a perturbation model that consists of a nominal model and bounds on real-valued structured and complex unstructured variations. Separation between parametric and unstructured uncertainty is achieved by first estimating low order dynamic models via frequency domain curve fitting followed by a linear Principle Component Analysis (PCA) [15]. The proposed linear PCA is a simplification of the nonlinear PCA used in [16], [17] solved with a non-convex optimization. However, the linear PCA allows to find the minimum number of independent perturbations in which the model parameters are varying with a straightforward singular value decomposition.

In addition, remaining differences between the low order parametric uncertainty model and the measured frequency responses are captured by a bounded unstructured uncertainty on a frequency dependent dual-Youla parameter. An unstructured dual-Youla uncertainty model can use prior information on a stabilizing feedback controller, creating an uncertainty model that is guaranteed to be stabilized by the feedback controller [18], [19]. The unstructured dual-Youla uncertainty model is known to be less conservative [20] in describing unstructured model uncertainty compared to standard additive or multiplicative uncertainty models.

II. EXPERIMENTAL DATA OF LTO SERVO ACTUATOR

The motivation for the work on uncertainty modeling in this paper comes from measured frequency domain data from several servo actuators used in data track following in Linear Tape Open (LTO) drives. In track following for an LTO drive [12], a magnetic flexible tape runs at variable speed along a magnetic read/write head and a digital position error signal (PES) is decoded from dedicated servo tracks on a flexible tape using a timing-based servo pattern. The digital PES is fed back to an digital embedded servo controller to generate

control signals for an LTO servo actuator via Zero Order Hold (ZOH) Digital to Analog Converter (DAC) amplifier to move the read/write head and follow the dedicated servo track despite Lateral Tape Movement (LTM). Hence, the PES is available only when the servo actuator is able to follow the dedicated servo track on the flexible tape in a feedback connection similar to Figure 1.

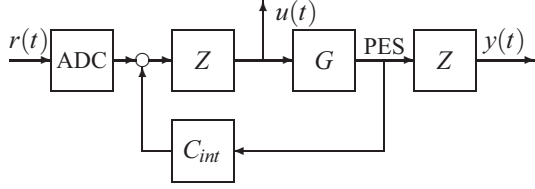


Fig. 1. Schematics of closed-loop data and closed-loop experiments for the uncertainty modeling and robust control of LTO drives

In Figure 1, G is used to indicate the servo actuator, C_{int} denoted the embedded servo controller and Z denotes a ZOH DAC conversion. For computing an estimate of the frequency response $\mathcal{G}(j\omega)$ of the servo actuator G , the feedback loop is augmented with an external reference signal $r(t)$ via an Analog to Digital Converter (ADC), a measurement of the input signal $u(t)$ to the actuator and an external measurement of the digital PES $y(t)$ via ZOH DAC [14]. Important for the discussion in this paper is that there exists information on a stabilizing controller C_{int} used in the closed-loop experiments.

Referring again to the closed-loop experiment in Figure 1, frequency domain data $\mathcal{G}(j\omega)$ of the servo actuator G can be obtained via closed-loop spectral analysis [21]. Using the notation $\Phi_{yr}(j\omega)$ to indicate the cross-spectral density function between $r(t)$ and $y(t)$, the estimate

$$\hat{\Phi}_{yr}(j\omega) = \frac{\sum_{k=1}^p Y_k(\omega) R_k^*(\omega)}{\sum_{k=1}^p R_k(\omega) R_k^*(\omega)}$$

where $Y_k(\omega) = \sum_{t=1}^N y_k(t) e^{-j\omega t}$ and $R_k(\omega) = \sum_{t=1}^N r_k(t) e^{-j\omega t}$ is found via the Welch method of averaging an N -point Fourier transforms [21] of the signals $y_k(t)$ and $r_k(t)$ for different experiments k . Based on this estimate we can formulate an estimate of the frequency domain data $\mathcal{G}(j\omega)$ of the servo actuator G via

$$\mathcal{G}(j\omega) = Z(j\omega)^{-1} \frac{\hat{\Phi}_{yr}(j\omega)}{\hat{\Phi}_{ur}(j\omega)} \quad (1)$$

where $Z(j\omega)$ denotes the known frequency response of a ZOH DAC. The amplitude Bode response of the estimate $\mathcal{G}_i(j\omega)$ in (1) from 15 different experiments has been depicted in Figure 2.

The experimental data in Figure 2 is computed based on experimental data from several (mechanically equivalent) servo actuators mounted in different LTO drives reflecting manufacturing tolerances. Due to contact between the servo head and the flexible tape, actuator dynamics varies depending on the tape manufacturing and flexibility. For operational condition variations, LTO drives were placed in a temperature controlled chamber where the temperature is varied

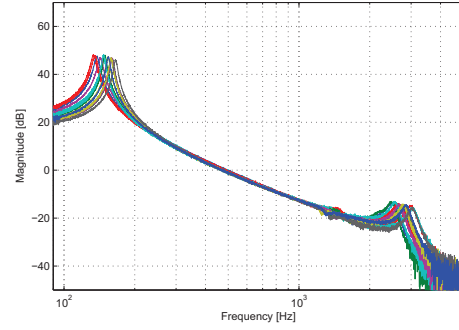


Fig. 2. Magnitude Bode plot of estimated frequency responses $\mathcal{G}(j\omega)$ in (1) for $i = 1, 2, \dots, 15$ different experimental conditions.

from 15 to 50 degree Celcius to account for changes in tape and actuator flexibility. We can see from Figure 2 that there are perturbations in the two main resonance modes around 150Hz and 2.5kHz and changes in the frequency range 1-2kHz. These variations will be modeled via structured and unstructured model perturbations.

III. STRUCTURED PARAMETER PERTURBATION

A. Linear parameter perturbation model

To address the structural perturbations observed in the resonance modes of the servo actuators, first low order continuous-time linear parameter models $G(s, \theta_i)$ parametrized via

$$G(s, \theta_i) = \frac{b_0^{(i)} + b_1^{(i)} s + \dots + b_m^{(i)} s^m}{1 + a_1^{(i)} s + \dots + a_n^{(i)} s^n}, \quad n \geq m$$

are estimated via standard frequency domain curve fitting

$$\hat{\theta}_i = \arg \min_{\theta_i} \| (\mathcal{G}_i(j\omega) - G(j\omega, \theta_i)) W_i(\omega) \|_2 \quad (2)$$

using the corresponding frequency domain data $\mathcal{G}_i(j\omega)$ and a frequency dependent weighting $W_i(\omega)$ that emphasizes the observed resonance frequencies in the data $\mathcal{G}_i(j\omega)$. The minimization in (2) is solved via iterative least-squares optimization [22] to find the parametric variations on the estimated parameter

$$\hat{\theta}_i = [b_0^{(i)} \quad b_1^{(i)} \quad \dots \quad b_m^{(i)} \quad a_1^{(i)} \quad \dots \quad a_n^{(i)}]^T \in \mathbb{R}^{p \times 1}$$

for $i = 1, 2, \dots, N$, where N is used to denote the number of frequency response measurements.

To characterize the parametric variations, we define the infinity mean $\bar{\theta}$:

$$\bar{\theta} = [\bar{b}_0 \quad \bar{b}_1 \quad \dots \quad \bar{b}_m \quad \bar{a}_1 \quad \dots \quad \bar{a}_n]^T \in \mathbb{R}^{p \times 1} \quad (3)$$

that minimizes the maximum distance between equivalent parameter coefficients and can be computed via

$$\bar{b}_l = \frac{\max_i b_l^{(i)} + \min_i b_l^{(i)}}{2}, \quad \bar{a}_k = \frac{\max_i a_k^{(i)} + \min_i a_k^{(i)}}{2}$$

$$\forall i = 1, 2, \dots, N, \quad l = 0, 1, \dots, m, \quad k = 1, 2, \dots, n$$

and define a parameter perturbation $\tilde{\theta}$ as

$$\tilde{\theta} = \hat{\theta}_i - \bar{\theta} \in \mathbb{R}^{p \times 1} \quad (4)$$

Denote $\hat{\theta}_i(k)$ to be the k^{th} element in the vector $\hat{\theta}_i$, then the bound $\gamma_k = \max_i |\hat{\theta}_i(k)|$ allows a parameter perturbation set to be defined as

$$\mathcal{S}_{\tilde{\theta}} = \{\tilde{\theta} : |\tilde{\theta}(k)| \leq \gamma_k, \forall k = 1, 2, \dots, p\} \quad (5)$$

resulting in a linear parametric perturbation model

$$\mathcal{P}_{\tilde{\theta}} = \left\{ G_{\tilde{\theta}} : G_{\tilde{\theta}} = \frac{\bar{B}(s) + \mathbb{B}(s)\tilde{\theta}}{A(s) + \mathbb{A}(s)\tilde{\theta}}, \tilde{\theta} \in \mathcal{S}_{\tilde{\theta}} \right\} \quad (6)$$

where $\mathcal{S}_{\tilde{\theta}}$ is given in (5) and

$$\begin{aligned} \bar{B}(s) &= \bar{b}_0 + \bar{b}_1 s + \dots + \bar{b}_m s^m \\ A(s) &= 1 + \bar{a}_1 s + \dots + \bar{a}_n s^n \\ \mathbb{B}(s) &= [1 \quad s \quad \dots \quad s^m \quad 0 \quad \dots \quad 0] \in \mathbb{C}^{1 \times p} \\ \mathbb{A}(s) &= [0 \quad 0 \quad \dots \quad s \quad \dots \quad s^n] \in \mathbb{C}^{1 \times p} \end{aligned} \quad (7)$$

Although (6) would model the parametric variations in the measured frequency responses $\mathcal{G}_i(j\omega)$, the bound γ_k in (5) allows each element $\tilde{\theta}_i(k)$ of the vector $\tilde{\theta}$ to vary independently. The variations of $\tilde{\theta}_i$ in (4) might be structured, especially when parameters vary jointly to find a less conservative uncertainty description.

B. Lower dimensional parameter perturbation

Reduction of the number of independent perturbations that occur in the variations of $\tilde{\theta}_i$ in (4) can be determined via a linear Principle Component Analysis (PCA) [15]. Although there may be non-affine structures of parameter dependence that could be solved via non-linear PCA [17], a linear PCA can be solved with a straightforward Singular Value Decomposition (SVD) or Eigenvalue Decomposition. Furthermore, any remaining differences between the frequency response of the parametric models $G(j\omega, \theta_i)$ and the frequency response data $\mathcal{G}_i(j\omega)$ will be bounded by an unstructured uncertainty.

For setting up the PCA, we first define a parameter perturbation matrix

$$\tilde{\Theta} = [\tilde{\theta}_1 \quad \tilde{\theta}_2 \quad \dots \quad \tilde{\theta}_N] \in \mathbb{R}^{p \times N} \quad (8)$$

from the N parameter estimates $\hat{\theta}_i \in \mathbb{R}^{p \times 1}$ and the infinity mean $\bar{\theta}$ in (3). Based on the matrix $\tilde{\Theta}$, two main steps are performed to reduce the variations of $\tilde{\theta}_i$ in (4) to a finite number $r \leq p$ of independent perturbations via the principle directions computed via PCA. The two steps are summarized in the following.

1) *Determination of number of principal components:* To find the principle directions regardless of the relative size of the perturbations, first the parameter perturbation matrix $\tilde{\Theta}$ in (8) is scaled to

$$\tilde{\Theta}^{(s)} = [\tilde{\theta}_1^{(s)} \quad \tilde{\theta}_2^{(s)} \quad \dots \quad \tilde{\theta}_N^{(s)}] \in \mathbb{R}^{p \times N} \quad (9)$$

where $\tilde{\theta}_i^{(s)}(k) = \tilde{\theta}_i(k)/\bar{\theta}_i(k); \forall i = 1, 2, \dots, N; k = 1, 2, \dots, p$ which means each parameter is scaled by its own nominal value. So the relative difference between the observed variations in $\hat{\theta}_i \in \mathbb{R}^{p \times 1}$ is normalized. Based on the scaled parameter perturbation matrix $\tilde{\Theta}^{(s)}$ we now define a scaled covariance matrix

$$C_{\tilde{\theta}}^{(s)} = \frac{1}{N} \tilde{\Theta}^{(s)} \tilde{\Theta}^{(s)T} \in \mathbb{R}^{p \times p} \quad (10)$$

and perform a SVD on to rewrite $C_{\tilde{\theta}}^{(s)}$ as

$$C_{\tilde{\theta}}^{(s)} = \begin{bmatrix} T^{(s)} & T_s^{(s)} \end{bmatrix} \begin{bmatrix} C_{\sigma}^{(s)} & 0 \\ 0 & C_s^{(s)} \end{bmatrix} \begin{bmatrix} T^{(s)} \\ T_s^{(s)} \end{bmatrix} \quad (11)$$

where the singular values of $C_{\tilde{\theta}}^{(s)}$ are separated into r large singular values in $C_{\sigma}^{(s)}$ and $p-r$ small singular values in $C_s^{(s)}$. With the separation of singular values we have

$$\arg \min_C \|C_{\tilde{\theta}}^{(s)} - C\|_F = T^{(s)} C_{\sigma}^{(s)} T^{(s)} \quad (12)$$

where C is a symmetric rank r matrix. The direct relation between Frobenius-norm minimization in (12) and the truncation of the SVD of the scaled covariance matrix $C_{\tilde{\theta}}^{(s)}$ makes the choice $r \leq p$ a well-motivated choice for the number of independent principle directions for the parameter perturbations.

2) *Least Squares optimization:* For parameter perturbation matrix $\tilde{\Theta}$ in (8) we can also define an (unscaled) covariance matrix $C_{\tilde{\theta}} = \frac{1}{N} \tilde{\Theta} \tilde{\Theta}^T \in \mathbb{R}^{p \times p}$. Knowing the number $r \leq p$ of principal components from the *scaled* covariance matrix in the first step, we perform again a SVD and use the number r to partition the SVD via

$$C_{\tilde{\theta}} = \begin{bmatrix} T & T_s \end{bmatrix} \begin{bmatrix} C_{\sigma} & 0 \\ 0 & C_s \end{bmatrix} \begin{bmatrix} T \\ T_s \end{bmatrix} \quad (13)$$

where $T \in \mathbb{R}^{p \times r}$. An similar approximation of $C_{\tilde{\theta}}$ by $TC_{\sigma}T^T$ where

$$C_{\sigma} = \frac{1}{N} \Sigma \Sigma^T \in \mathbb{R}^{r \times r} \quad (14)$$

would lead to an error $E = \tilde{\Theta} - T\Sigma$ on the parameter perturbation matrix $\tilde{\Theta}$ in (8). Instead of computing $\Sigma \in \mathbb{R}^{r \times N}$ from a Cholesky factorization of C_{σ} as in (14), a Least Squares (LS) minimization of $\|E\|_F$ is used to compute Σ . The optimal solution

$$\hat{\Sigma} = \arg \min_{\Sigma} \|\tilde{\Theta} - T\Sigma\|_F$$

is given by the standard LS solution

$$\hat{\Sigma} = (T^T T)^{-1} T^T \tilde{\Theta} \quad (15)$$

Defining

$$\hat{\Sigma} = [\hat{\sigma}_1 \quad \hat{\sigma}_2 \quad \dots \quad \hat{\sigma}_N] \in \mathbb{R}^{r \times N} \quad (16)$$

allows the parameter perturbations $\tilde{\theta}_i$ to be written as

$$\tilde{\theta}_i = T \hat{\sigma}_i + e_i; \quad i = 1, 2, \dots, N \quad (17)$$

where $T \in \mathbb{R}^{p \times r}$ and $\hat{\sigma}_i$ is a reduced size independent parameter perturbation of $r \times 1$ where $r \leq p$. The least squares minimization in (15) has minimized the 2-norm of the error e_i . The end result is a reduced size $r \times 1$ perturbation $\hat{\sigma}_i$ where T scales the perturbation on the $p \times 1$ parameter.

C. Reduced size linear parameter perturbation model

The PCA leads to the structural parameter variations in (17) that can be approximated by

$$\theta_i = \bar{\theta} + T\hat{\sigma}_i, \quad i = 1, 2, \dots, N \quad (18)$$

where $\bar{\theta} \in \mathbb{R}^{p \times 1}$ is the infinity mean given in (3), $T \in \mathbb{R}^{p \times r}$ is found from the SVD in (13) and $\hat{\sigma}_i \in \mathbb{R}^{r \times 1}$ is due to the LS optimization in (15) and the definition in (16). To write this in a standard structured parametric uncertainty model, consider the scaling of $\hat{\sigma}_i$ by the scaling matrix

$$S = \text{diag}(s_1, s_2, \dots, s_r) \in \mathbb{R}^{r \times r}, \\ s_k = \max_i |\hat{\sigma}_i(k)|, \quad k = 1, 2, \dots, r.$$

where $\hat{\sigma}_i(k)$ denotes the k th element of $\sigma_i \in \mathbb{R}^{r \times 1}$. This allows a reduced size $r \leq p$ parameter perturbation

$$\theta = \bar{\theta} + TS\delta, \quad \delta \in \mathcal{S}_\delta$$

where the reduced size linear parameter perturbation set \mathcal{S}_δ is defined as

$$\mathcal{S}_\delta = \{\delta : |\delta(k)| < 1, \forall k = 1, 2, \dots, r\} \quad (19)$$

in which $\delta(k)$ again denotes the k th element of $\delta \in \mathbb{R}^{r \times 1}$. The final result is a reduced size $r \leq p$ linear parametric perturbation model

$$\mathcal{P}_\delta = \left\{ G_\delta : G_\delta = \frac{\bar{B}(s) + \mathbb{V}_b(s)\delta}{A(s) + \mathbb{V}_a(s)\delta}, \delta \in \mathcal{S}_\delta \right\} \quad (20)$$

where \mathcal{S}_δ is given in (19) and

$$\mathbb{V}_b(s) = \mathbb{B}(s)TS \in \mathbb{C}^{1 \times r} \\ \mathbb{V}_a(s) = \mathbb{A}(s)TS \in \mathbb{C}^{1 \times r}$$

and $\mathbb{B}(s)$, $\mathbb{A}(s)$ were defined previously in (7).

D. Application to LTO tape data

Based on the 15 measured frequency responses depicted in Figure 2, continuous-time linear parametric models

$$G(s, \theta_i) = \frac{b_0^{(i)} + b_1^{(i)}s + b_2^{(i)}s^2 + b_3^{(i)}s^3}{1 + a_1^{(i)}s + a_2^{(i)}s^2 + a_3^{(i)}s^3 + a_4^{(i)}s^4}$$

are fitted to capture the structural variations in the main resonance modes around 150Hz and 2.5kHz. Although a relative degree of 2 is able to fit most of the frequency domain data, a relative degree of 1 with a third order numerator is used to find the best strictly proper fourth order model. The fourth order models lead to parameter estimates $\hat{\theta}_i \in \mathbb{R}^{p \times 1}$ with $p = 8$ and application of the linear PCA allows the structural parameter variations in $\hat{\theta}_i$ to be approximated by (18) using $T \in \mathbb{R}^{p \times r}$ where $r = 4$. The structural parameter variations can be reduced to a smaller size $r \leq p$ is likely due to changes in resonance frequency only, while little change in damping is observed in the main resonance modes around 150Hz and 2.5kHz.

Varying the $r \times 1$ perturbation δ within the normalized bounds $|\delta(k)| < 1$ in the linear parametric perturbation model of (20) now allows the structural variations in the servo actuators to be modeled. This has been demonstrated in

Figure 3, where the amplitude Bode plot of 50 randomly chosen models from the linear parametric perturbation model of (20) has been plotted. It can be observed that the structural variations in the resonance modes have been captured by the model defined in (20) for $|\delta(k)| < 1$.

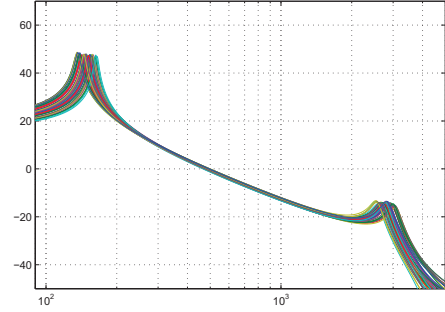


Fig. 3. Magnitude plot of 50 randomly chosen models $|G_\delta(j\omega)|$ from the linear parametric perturbation model of (20)

IV. UNSTRUCTURED UNCERTAINTY CHARACTERIZATION

A. Dual-Youla uncertainty

Inevitably, some differences between the modeled frequency response $G(j\omega, \theta_i)$, with θ_i given in (18), and the measured frequency response $\mathcal{G}_i(j\omega)$ remain. These difference may be due to the approximation of θ_i by a reduced size $r \leq p$ of structural perturbation as indicated by (18) or due to remaining unmodeled dynamics during the curve fitting. The remaining difference are bounded by an unstructured uncertainty on a dual-Youla parameter that uses prior information on a stabilizing feedback controller.

The dual-Youla parametrization allows the parametrization of all models stabilized by a given feedback controller by the requirement of a stable dual-Youla parameter [18], [19]. The stability requirement on the dual-Youla parameter can also be used in bounding model perturbations to formulate closed-loop unstructured uncertainty models that are known to be less conservative than standard open-loop uncertainty models [20].

With C_{int} stabilizing all measured servo actuators, we assume and verify that C_{int} also stabilizes all models $G(\theta_i)$, $i = 1, 2, \dots, N$. According to the dual-Youla parametrization, for each servo actuator \mathcal{G}_i there exists a $\Delta_i \in RH_\infty$ that satisfies

$$\mathcal{N}_i = N_i + \Delta_i D_C \\ \mathcal{D}_i = D_i + \Delta_i N_C \quad (21)$$

where $(\mathcal{N}_i, \mathcal{D}_i)$ is the (unknown) right coprime factor of \mathcal{G}_i , (N_i, D_i) is the (known) right co-prime factor of the model $G(\theta_i)$ and (N_C, D_C) is (known) right coprime factor of C_{int} . Knowing (N_i, D_i) , (N_C, D_C) and \mathcal{G}_i one can compute Δ_i explicitly via $\Delta_i = D_C^{-1}(1 + \mathcal{G}_i C_{int})^{-1}(\mathcal{G}_i - G(\theta_i))D_i$. For a stable controller C_{int} we may choose $N_C = C_{int}$ and $D_C = I$. Similarly, for a stable model $G(\theta_i)$ we may choose $N_i = G(\theta_i)$ and $D_i = I$, simplifying the explicit expression for Δ_i to $\Delta_i = (1 + \mathcal{G}_i C_{int})^{-1}(\mathcal{G}_i - G(\theta_i))$. It should be pointed out that $\Delta_i \in RH_\infty$ due to the dual-Youla parametrization. With frequency domain measurements $\mathcal{G}_i(j\omega)$ we can formulate

an upper bound for the unknown, but stable unstructured uncertainty

$$\Delta_i(j\omega) = (1 + \mathcal{G}_i(j\omega)C_{int}(j\omega))^{-1}(\mathcal{G}_i(j\omega) - G(j\omega, \theta_i))$$

Defining

$$\Delta_u(\omega) = \max_i |\Delta_i(\omega)| \quad \forall \omega, i = 1, 2, \dots, N \quad (22)$$

an unstructured dual-Youla uncertainty model set can be formulated via

$$\mathcal{P}_\Delta = \{G_\Delta : G_\Delta = (G(\theta_i) + \Delta W)(I - \Delta WC_{int})^{-1}, |\Delta| < 1\} \quad (23)$$

where $W(j\omega)$ is a stable and stable invertible filter that overbounds $\Delta_u(\omega)$ in (22) via $|\Delta_u(\omega)W^{-1}(j\omega)|_\infty < 1$.

B. Application to LTO tape data

Computation of $\Delta_i(j\omega)$ for every fourth order model $G(\theta_i)$ contained in (20) and obtained from curve fitting followed by PCA allows the computation of frequency dependent $\Delta_u(\omega)$ in (22) and has been depicted in Figure 4. As a frame of reference, in Figure 4 also the results are plotted in case *only* an additive uncertainty or dual-Youla unstructured uncertainty (DY) is used without modeling the structural perturbations. Clearly, the additional step of extracting structural uncertainty via curve fitting and a PCA reduces the remaining unstructured uncertainty.

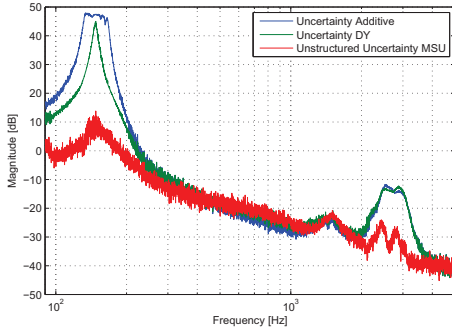


Fig. 4. Comparison of frequency dependent unstructured uncertainties when using only Additive uncertainty, only Dual-Youla (DY) uncertainty or the Mixed Structured and Unstructured (MSU) uncertainty

V. MIXED STRUCTURED AND UNSTRUCTURED UNCERTAINTY IN LFT FORM

The model set of structured perturbations \mathcal{P}_δ in (20) with $\Delta_s = \text{diag}(\delta)$ can be also written into an upper LFT $\mathcal{F}_u(P, \Delta_s) = P_{22} + P_{21}\Delta_s(1 - P_{11}\Delta_s)^{-1}P_{12}$ where the entries of the 2×2 block transfer matrix P are given by

$$\begin{aligned} P_{11} &= \begin{bmatrix} -\bar{A}^{-1}\nabla_a \\ \vdots \\ -\bar{A}^{-1}\nabla_a \end{bmatrix} & P_{12} &= \begin{bmatrix} \bar{A}^{-1} \\ \vdots \\ \bar{A}^{-1} \end{bmatrix} \\ P_{21} &= \nabla_b - \bar{B}\bar{A}^{-1}\nabla_a & P_{22} &= \bar{B}\bar{A}^{-1} \end{aligned}$$

Similarly, the model set of unstructured perturbations \mathcal{P}_Δ in (23) can be written in an upper LFT $\mathcal{F}_u(Q, \Delta) = Q_{22} +$

$Q_{21}\Delta(1 - Q_{11}\Delta)^{-1}Q_{12}$ where the entries of the 2×2 block transfer matrix Q are given by

$$\begin{aligned} Q_{11} &= WC_{int} & Q_{12} &= W \\ Q_{21} &= I + G(\theta_i)C_{int} & Q_{22} &= G(\theta_i) \end{aligned}$$

If the above mentioned LFTs $\mathcal{F}_u(P, \Delta_s)$ and $\mathcal{F}_u(Q, \Delta)$ are combined by stacking Δ_s and Δ diagonally, a Mixed Structured and Unstructured (MSU) perturbation model in the form of an upper LFT $\mathcal{F}_u(\tilde{P}, \text{diag}(\delta, \Delta))$ is formed. The resulting MSU perturbation model is summarized by

$$\mathcal{P}_{\delta, \Delta} = \{G_{\delta, \Delta} : G_{\delta, \Delta} = \mathcal{F}_u(\tilde{P}, \text{diag}(\delta, \Delta)) \mid |\delta(k)| < 1, \|\Delta(\omega)\|_\infty < 1, k = 1, 2, \dots, r\} \quad (24)$$

where the entries of the 2×2 block transfer matrix \tilde{P} are given by

$$\begin{aligned} \tilde{P}_{11} &= \begin{bmatrix} P_{11} & P_{12}C_{int} \\ 0 & WC_{int} \end{bmatrix} & \tilde{P}_{12} &= \begin{bmatrix} P_{12} \\ W \end{bmatrix} \\ \tilde{P}_{21} &= \begin{bmatrix} P_{21} & I + P_{22}C_{int} \end{bmatrix} & \tilde{P}_{22} &= P_{22} \end{aligned} \quad (25)$$

VI. PERFORMANCE ROBUSTNESS

A. Robust Performance Test

For formulating a test on performance robustness, first a definition on (nominal) performance must be given. To facilitate the use of the main loop theorem [1], nominal performance of the servo actuators in an LTO drive is specified as an weighted H_∞ criterion on the disturbance rejection function $(I + CG)^{-1}$. Defining an error signal $e = W_s(d + y)$ and augmenting the LFT $y = \mathcal{F}_u(\tilde{P}, \text{diag}(\delta, \Delta))u$ with a feedback connection $u = -C(d + y)$ leads to an LFT $e = \mathcal{F}_u(M, \text{diag}(\delta, \Delta))d$ for the relation between the error signal e and disturbance signal d . Performance robustness can now be verified with the main loop theorem and using the computation of a structured singular value $\mu_\Delta(\cdot)$ with respect to the perturbation structure

$$\Delta = \{\text{diag}(\delta(1), \delta(2), \dots, \delta(r), \Delta, \Delta_f) : \delta(k) \in \mathbb{R}, \Delta, \Delta_f \in \mathbb{C}\} \quad (26)$$

of the mixed r dimensional (real) $\text{diag}(\delta)$ and a 2 dimensional complex uncertainty structure $\text{diag}(\Delta, \Delta_f)$.

Theorem 1: Robust Performance [1]

Consider \tilde{P} given in (25) and let

$$M = \begin{bmatrix} M_{11} & -\tilde{P}_{12}M_{22} \\ W_s M_{22} C \tilde{P}_{21} & W_s M_{22} \end{bmatrix}$$

where $M_{11} = \mathcal{F}_l(\tilde{P}, -C)$, $M_{22} = (I + C\tilde{P}_{22})^{-1}$ and consider models $G_{\delta, \Delta} \in \mathcal{P}_{\delta, \Delta}$ given in (24). The negative feedback connection of C and $G_{\delta, \Delta}$ is robustly stable and the H_∞ performance specification $\|\mathcal{F}_u(M, \text{diag}(\delta, \Delta))\|_\infty \leq 1$ is satisfied all $G_{\delta, \Delta} \in \mathcal{P}_{\delta, \Delta}$ iff $\mu_\Delta(M) < 1$ computed with respect to the perturbation structure Δ defined in (26).

As computation of $\mu_\Delta(M)$ is in general NP-hard, overbounds can only be computed by a frequency point wise evaluation of $\mu_\Delta(M(j\omega))$ over a frequency grid $\omega \in \Omega$ [1]. Such frequency dependent overbounds can still be used to check if $\mu_\Delta(M(j\omega)) < 1 \quad \forall \omega \in \Omega$ and robust performance can be verified provided the frequency grid Ω is chosen to be dense.

B. Robust performance test for LTO actuator data

The robust performance test summarized in Theorem 1 is a much stronger requirement than only robust stability. For testing performance robustness based on the mixed structured and unstructured perturbation (MSU) model $\mathcal{P}_{\delta,\Delta}$ given in (24) and determined from the 15 frequency responses given in Figure 2, a performance weighting function W_s on the disturbance rejection function $(I + CG)^{-1}$ was chosen. Randomly selecting 50 different models $G_{\delta,\Delta} \in \mathcal{P}_{\delta,\Delta}$ and computing the amplitude of $|(I + CG_{\delta,\Delta})^{-1}|$ leads to the amplitude Bode plot depicted in Figure 5.

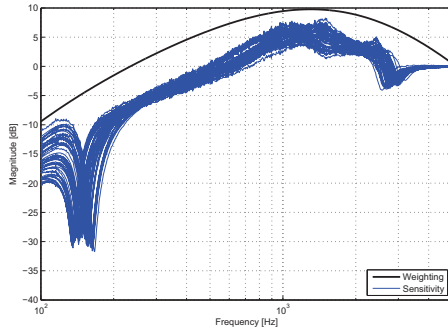


Fig. 5. Amplitude Bode plot of the error rejection for 50 randomly chosen models from the Mixed Structured and Unstructured (MSU) perturbation model given in (24) compared to the performance weighting function W_s .

The result indicate that all chosen models satisfy the H_∞ -norm based performance specification due to W_s overbounding all 50 error rejection functions. The results is formally proven by the computation of the (upper bound) of $\mu_\Delta(M)$ in Figure 6. As a frame of reference, in Figure 6 also the robust performance results are plotted in case *only* an additive uncertainty or dual-Youla unstructured uncertainty (DY) is used without modeling the structural perturbations and indicate that $\mu > 1$ for those uncertainty descriptions. Clearly, the Mixed Structured and Unstructured (MSU) perturbation model $\mathcal{P}_{\delta,\Delta}$ given in (24) yields less conservative results when checking performance robustness.

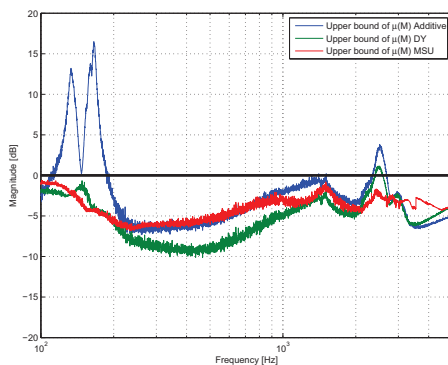


Fig. 6. Comparison of μ -based robust performance test when using only Additive uncertainty, only Dual-Youla (DY) uncertainty or the Mixed Structured and Unstructured (MSU) uncertainty

VII. CONCLUSIONS

Starting from multiple frequency domain measurements, this paper presents a procedure to formulate a mixed structured and unstructured perturbation model. A separation between parametric and unstructured uncertainty is achieved

by first estimating low order linear parameter models via frequency domain curve fitting followed by a linear Principle Component Analysis (PCA). Remaining differences are bounded by unstructured uncertainty on a dual-Youla parameter that uses prior information on a stabilizing feedback controller. The favorable properties of the perturbation model is demonstrated via a performance robustness test applied to data from servo actuators in Linear Tape Open (LTO) drives.

REFERENCES

- [1] K. Zhou and J. Doyle, *Essentials of Robust Control*. Upper Saddle River, NJ: Prentice Hall, 1997.
- [2] M. Green and D. Limebeer, *Linear Robust Control*. Mineola, NY: Dover, 2012.
- [3] T. Zhou and H. Kimura, "Simultaneous identification of nominal model, parametric uncertainty and unstructured uncertainty for robust control," *Automatica*, vol. 30, pp. 391–402, 1994.
- [4] J. Chen and G. Gu, *Control Oriented System Identification: An \mathcal{H}_∞ Approach*. Hoboken, NJ: Wiley, 2000.
- [5] R. Smith and J. Doyle, "Model validation: A connection between robust control and identification," *IEEE Tran. on Automatic Control*, vol. 37, pp. 942–952, 1992.
- [6] G. Rodonyi, B. Lantos, and J. Bokor, "Uncertainty modeling and robust control of LTI systems based on integral quadratic constraints," in *Proc. 11th Int. Conf. On Intel. Eng. Systems*, 2007, pp. 207–212.
- [7] F. Chavez and D. Schmidt, "Uncertainty modeling for multivariable-control robustness analysis of elastic high-speed vehicles," *Journal of Guidance Control and Dynamics*, vol. 22, pp. 87–95, 1999.
- [8] R. de Callafon, R. Nagamune, and R. Horowitz, "Robust dynamic modeling and control of dual-stage actuators," *IEEE Tran. on Mag.*, vol. 42, no. 2, pp. 247–254, 2006.
- [9] R. Conway, S. Felix, and R. Horowitz, "Model reduction and parametric uncertainty identification for robust control synthesis for dual-stage hard disk drives," *IEEE Tran. on Mag.*, vol. 43, pp. 3763–3768, 2007.
- [10] R. Kosut, M. Lau, S. Boyd, I. Inc, and C. Santa Clara, "Set-membership identification of systems with parametric and nonparametric uncertainty," *IEEE Tran. on Automatic Control*, vol. 37, pp. 929–941, 1992.
- [11] A. Pantazi, J. Jelitto, and E. Bui, N. Ans Eleftheriou, "Track-follow control for tape storage," in *Proc. 5th IFAC Symp. Mechatronics Systems*, Cambridge, MA, 2010, pp. 532–537.
- [12] G. Cherubini, R. Cideciyan, L. Dellmann, E. Eleftheriou, W. Haeberle, J. Jelitto, V. Kartik, M. Lantz, S. Ölçer, A. Pantazi, H. Rothuizen, D. Berman, W. Imano, P. Jubert, G. McClelland, P. Koeppel, K. Tsuruta, T. Harasawa, Y. Murata, A. Musha, H. Noguchi, H. Ohtsu, O. Shimizu, and R. Suzuki, "29.5-Gb/in² recording areal density on Barium Ferrite tape," *IEEE Tran. on Mag.*, vol. 47, pp. 137–147, 2011.
- [13] V. Kartik, A. Pantazi, and M. Lantz, "Track-following high frequency lateral motion of flexible magnetic media with sub-100 nm positioning error," *IEEE Tran. of Mag.*, vol. 47, pp. 1868–1873, 2011.
- [14] M. Briegel and R. Rijkers, "Uncertainty modeling and robust control of linear tape-open drives," Eindhoven University of Technology, Tech. Rep., 2010, <http://www.mate.tue.nl/mate/pdfs/11797.pdf>.
- [15] I. Jolliffe, *Principal Component Analysis*. NY, NY: Springer, 2002.
- [16] R. Nagamune and J. Choi, "Parameter reduction in estimated model sets for robust control," *ASME Journal Dyn. Syst., Meas., Control*, vol. 132, 2010.
- [17] M. Sepasi, F. Sassani, and R. Nagamune, "Parameter uncertainty modeling using the multidimensional principal curves," *Journal of Dyn. Sys., Meas., Control*, vol. 132, 2010.
- [18] B. Anderson, "From Youla-Kucera to identification, adaptive and nonlinear control," *Automatica*, vol. 34, pp. 1485–1506, 1998.
- [19] H. Niemann, "Dual Youla parameterisation," *IEE Proc. Control Theory Appl.*, vol. 150, pp. 493–497, 2003.
- [20] S. Douma, P. Van den Hof, and O. Bosgra, "Controller tuning freedom under plant identification uncertainty: Double youla beats gap in robust stability," *Automatica*, vol. 39, pp. 325–333, 2003.
- [21] L. Ljung, *System Identification: Theory for the User (2nd Edition)*. Upper Saddle River, NJ: Prentice Hall, 1999.
- [22] R. de Callafon, D. Roover, and P. Van den Hof, "Multivariable least squares frequency domain identification using polynomial matrix fraction descriptions," in *Proc. 35th IEEE Conf. On Decision and Control*, Kobe, Japan, 1996, pp. 2030–2035.